Vol. 29 (1998) ACTA PHYSICA POLONICA B No 5

POLARIZED PARTON DISTRIBUTIONS AND QCD SPIN TESTS AT RHIC-BNL*

J. Soffer

Centre de Physique Théorique, CNRS Luminy
Case 907, F-13288 Marseille Cedex 09, France

(Received February 13, 1998)

The RHIC facility at BNL will be operating soon, part of the year, as a polarized proton-proton collider. This will allow the undertaking of a vast spin physics programme, mainly by the two large detectors PHENIX and STAR. We review some theoretical aspects of this research programme which will allow, firstly to improve our present knowledge on polarized quark, gluon and sea distributions in a nucleon, secondly to perform novel QCD spin tests and finally, perhaps, to uncover some new physics.

PACS numbers: 13.60. –r, 13.60. Hb, 13.88. +e, 14.20. Dh

1. Introduction

Considerable progress have been made over the last ten years or so, in our understanding of the spin structure of the nucleon. This is essentially due to a better determination of the polarized structure functions $g_1^{p,n,d}(x,Q^2)$, from polarized Deep-Inelastic-Scattering (DIS) on different targets (Hydrogen, Deuterium, Helium-3). However these fixed polarized targets experiments [1], performed at CERN, DESY and SLAC, cover only a limited kinematic region, that is $0.005 \leq x \leq 0.7$, with the corresponding average $< Q^2 >$ between $2\,\mathrm{GeV}^2$ and $10\,\mathrm{GeV}^2$. In spite of the constant progress realized in the accuracy of the data, they can still be described, non uniquely, in terms of several sets of polarized parton distributions. In particular, sea quark, antiquark and gluon distributions remain highly ambiguous. The restricted Q^2 range accessible by the data makes also rather difficult, sensible tests of the Q^2 evolution, predicted by recent higher order QCD calculations. Moreover it is not possible to obtain a good flavor separation, to isolate the contribution of each quark to the nucleon spin.

* Presented at the Cracow Epiphany Conference on Spin Effects in Particle Physics and Tempus Workshop, Cracow, Poland, January 9–11, 1998.

Polarized hadronic collisions, which are another way to investigate this research field, have accomplished little progress due to the scarcity of the data in appropriate kinematic regions, and a low energy range, so far accessible to very few dedicated experiments. Let us recall that the highest energy for studying polarized pp ($\bar{p}p$) collisions has been obtained at Fermilab by the E704 experiment [2] with a $200\,\mathrm{GeV}/c$ polarized proton (antiproton) beam on a fixed target, that is $\sqrt{s} = 19.4\,\mathrm{GeV}$. This situation will change drastically soon when the RHIC facility at BNL will start running, by 1999 or so, part of the time as a polarized pp collider. A vast spin programme will be undertaken by the two large detectors PHENIX and STAR, which will operate at RHIC and also by the $pp2pp$ experiment, dedicated to pp elastic and total cross sections. Before we go on and explain very briefly what will be done, let us recall three key parameters, which will be crucial to answer some of the very challenging questions. The proton beam polarization P will be maintained at the level of 70%, in both *longitudinal* and *transverse* directions, the center-of-mass energy $\sqrt{s}$ will be ranging between $100\,\mathrm{GeV}$ and $500\,\mathrm{GeV}$ and at its maximum value, the luminosity is expected to reach $L = 2.10^{32}\,\mathrm{cm}^{-2}\,\mathrm{sec}^{-1}$.

The *Siberian snakes* magnets which preserve the degree of polarization in the RHIC main rings and the *spin rotators* which select the beam spin direction, are under construction thanks to a substantial financial contribution from the Japanese Institute RIKEN in collaboration with BNL. The high luminosity will allow very copious effective yields for different reactions (γ, jet, $W^{\pm}$ production, *etc...*) and therefore the measurement of the corresponding spin asymmetries will be made to a very good level of accuracy, in the kinematic regions relevant for QCD spin tests. The spin programme at RHIC will provide answers to fundamental questions which will be listed now in turn.

In the next section we will recall some basic definitions of the helicity asymmetries. Section 3 will be devoted to prompt photon production and jet production, which will allow the first direct determination of the gluon helicity distribution $\Delta G(x, Q^2)$ inside a polarized nucleon. Next we will show in Section 4, how antiquark helicity distributions $\Delta\bar{q}(x, Q^2)$ can be isolated in $W^{\pm}$ production, which leads also to the u-d flavor separation. This has been done, rather inaccurately, in semi-inclusive DIS. From transversely polarized proton beams, as we will see in Section 5, it is possible to make the first measurement of the transversity distributions $h_1^{q,\bar{q}}(x, Q^2)$ in Drell–Yan lepton pair production. Finally, in Section 6 we will indicate the relevance of the parity violating asymmetry in single jet production. It might provide a clean signature for new physics and, as an example, we will consider the possible effects of a quark-quark contact interaction.

2. Basic definitions and helicity asymmetries

Fundamental interactions at short distances which are explored in high energy hadronic collisions, involve hard scattering of quarks, antiquarks and gluons. Let us consider the general hadronic reaction

$$a + b \to c + X\,, \tag{1}$$

where c, in the cases we will consider below, is either a photon, a Z, a $W^{\pm}$ or a single-jet. In the hard scattering kinematic region, the cross section describing (1) reads in the QCD parton model, provided factorization holds, as

$$d\sigma(a+b \to c+X) = \sum_{ij} \frac{1}{1+\delta_{ij}} \int dx_a dx_b \left[f_i^{(a)}(x_a, Q^2) f_j^{(b)}(x_b, Q^2)\, d\hat{\sigma}^{ij} + (i \leftrightarrow j) \right]. \tag{2}$$

The summation runs over all contributing parton configurations, the $f(x, Q^2)$'s are the parton distributions, directly extracted from DIS for quarks and antiquarks and indirectly for gluons. Here $\mathrm{d}\hat{\sigma}_{ij}$ is the cross section for the interaction of two partons i and j which can be calculated perturbatively, some of which, at the lowest order, are given in Ref. [3]. If we consider the reaction (1) with *both* initial hadrons, a and b longitudinally polarized, one useful observable is the *double* helicity asymmetry A_{LL} defined as

$$A_{\mathrm{LL}} = \frac{d\sigma_{a(+)b(+)} - d\sigma_{a(+)b(-)}}{d\sigma_{a(+)b(+)} + d\sigma_{a(+)b(-)}}\,, \tag{3}$$

when we assume parity conservation, *i.e.* $\mathrm{d}\sigma_{a(\lambda)b(\lambda')} = \mathrm{d}\sigma_{a(-\lambda)b(-\lambda')}$. Its explicit expression, assuming factorization, is given by

$$A_{\mathrm{LL}} d\sigma = \sum_{ij} \frac{1}{1+\delta_{ij}} \int dx_a dx_b \left[\Delta f_i^{(a)}(x_a, Q^2) \Delta f_j^{(b)}(x_b, Q^2) \hat{a}_{\mathrm{LL}}^{ij} d\hat{\sigma}^{ij} + (i \leftrightarrow j) \right], \tag{4}$$

where $\mathrm{d}\sigma$ is given by Eq. (2) and $\hat{a}_{\mathrm{LL}}^{ij}$ denotes the corresponding subprocess double asymmetry for initial partons i and j. The Δf's are defined as

$$\Delta f(x, Q^2) \;=\; f_+(x, Q^2) \;-\; f_-(x, Q^2)\,, \tag{5}$$

where $f_{\pm}$ are the parton distributions in a polarized hadron with helicity either parallel (+) or antiparallel (-) to the parent hadron helicity. Recall that the unpolarized distributions are $f = f_+ + f_-$ and Δf measures how much the parton f "remembers" the parent hadron helicity. If the subprocess involves parity violating interactions, one can consider another interesting

observable which requires only *one* initial hadron polarized, that is the *single* helicity asymmetry $A_{\rm L}$, defined as

$$A_{\rm L} = \frac{d\sigma_{a(-)} - d\sigma_{a(+)}}{d\sigma_{a(-)} + d\sigma_{a(+)}}\,. \tag{6}$$

In addition, if both a and b are polarized one can also have two *double* helicity parity violating asymmetries defined as

$$A_{\rm LL}^{\rm PV} = \frac{d\sigma_{a(-)b(-)} - d\sigma_{a(+)b(+)}}{d\sigma_{a(-)b(-)} + d\sigma_{a(+)b(+)}} \;\text{ and }\; \bar{A}_{\rm LL}^{\rm PV} = \frac{d\sigma_{a(-)b(+)} - d\sigma_{a(+)b(-)}}{d\sigma_{a(-)b(+)} + d\sigma_{a(+)b(-)}}\,, \tag{7}$$

which can be simply related to $A_{\rm L}$ [4]. Several sets of polarized parton densities $\Delta f(x,Q^2)$ ($f = q, \bar{q}, G$) have been proposed in the recent literature [5-10]. Using some of these parametrizations to calculate helicity asymmetries for various processes, we will show how the RHIC-BNL spin programme will be able, in particular, to pin down the polarized helicity distributions which remain badly constrained by polarized DIS experiments.

3. How to pin down $\Delta G(x, Q^2)$?

The cross section for direct photon production on pp collisions at high $p_{\rm T}$ is considered as one of the cleanest probe of the unpolarized gluon distribution $G(x,Q^2)$. This is partly due to the fact that the photon originates in the hard scattering subprocess and is detected without undergoing fragmentation. Moreover in pp collisions the quark-gluon Compton subprocess $qG \to q\gamma$ dominates largely and the quark-antiquark annihilation subprocess $q\bar{q} \to G\gamma$ can be neglected. Consequently the double helicity asymmetry $A_{\rm LL}^{\gamma}$ (see Eq. (4)), which involves in this case only one subprocess, becomes particularly simple to calculate and is expected to be strongly sensitive to the sign and magnitude of $\Delta G(x,Q^2)$. For the Compton subprocess, $\hat{a}_{\rm LL}$ whose expression at the lowest order is given in Ref. [3], is always positive and such that $\hat{a}_{\rm LL}(\hat{\theta}_{\rm cm} = 90^\circ) = 3/5$ where $\hat{\theta}_{\rm cm}$ is the center of mass (c.m.) angle in the subprocess.

In Fig. 1 we show a complete comparison of the results we obtained for the $p_{\rm T}^{\gamma}$ distribution of $A_{\rm LL}^{\gamma}$, at pseudo rapidity $\eta = 0$, using the different sets of polarized parton distributions we have mentioned in the previous section, with a leading order Q^2 evolution. Actually we find that the smallest predictions are obtained from the sets Ref. [7] and Ref. [8] which have the smallest $\Delta G(x)/G(x)$. The predictions differ substantially at large $p_{\rm T}$, which corresponds to the region, say around $x = 0.4$ or so, where the distributions $\Delta G(x)$ have rather different shapes. We have also indicated the expected statistical errors based on an integrated luminosity $L = 800\ {\rm pb}^{-1}$ at

$\sqrt{s} = 500\,\mathrm{GeV}$, for three months running time. We have evaluated the event rates in the pseudo-rapidity gap $-1.5 < \eta < 1.5$, assuming a detector efficiency of 100% and for a p_{T}^{γ} acceptance $\Delta p_{\mathrm{T}}^{\gamma} = 5$ GeV/c. We see that up to $p_{\mathrm{T}}^{\gamma} = 50$ GeV/c or so, A_{LL}^{γ} will be determined with an error less than 5% which therefore will allow to distinguish between these different possible $\Delta G(x)$. For very large p_{T}^{γ}, the event rate drops too much to provide any sensitivity in the determination of $\Delta G(x)$. The pseudo-rapidity distribution of $A_{\mathrm{LL}}^{\gamma}(\eta)$ at a fixed p_{T}^{γ} value has been also calculated in Ref. ([10]) and it shows a systematic increase of A_{LL}^{γ} for higher η.

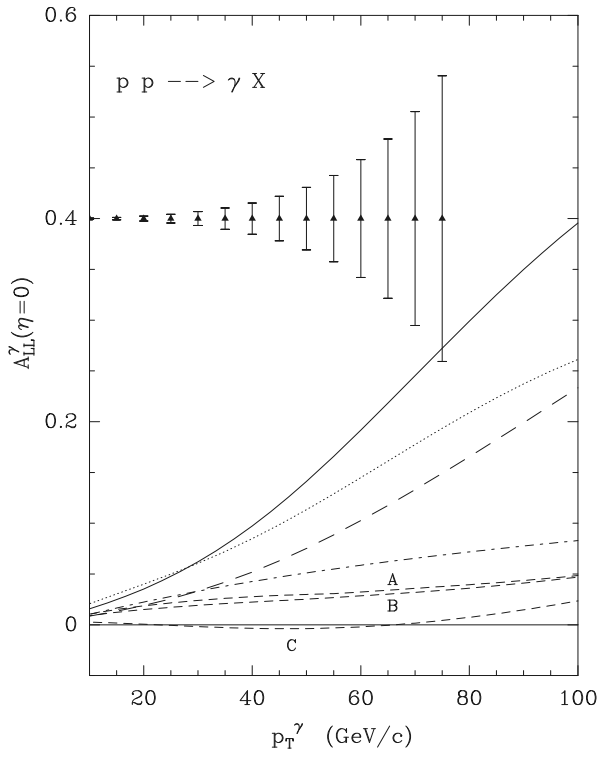

Fig. 1. The double helicity asymmetry $A_{\mathrm{LL}}^{\gamma}(\eta = 0)$ at $\eta = 0$ versus p_{T}^{γ} for $\sqrt{s} = 500\,\mathrm{GeV}$ calculated with different parton densities. (Solid and large dashed curves [5], dotted curve [6], dashed-dotted curve [8], small dashed curves [7].) (Taken from Ref. [10].)

Inclusive jet production is also a physics area where one can learn a lot about parton densities and, considering the vast amount of unpolarized existing data, it has been regarded as an important QCD testing ground. Event rates are much larger than for prompt photon production, but there is a drawback because many subprocesses are involved, unlike in the previous

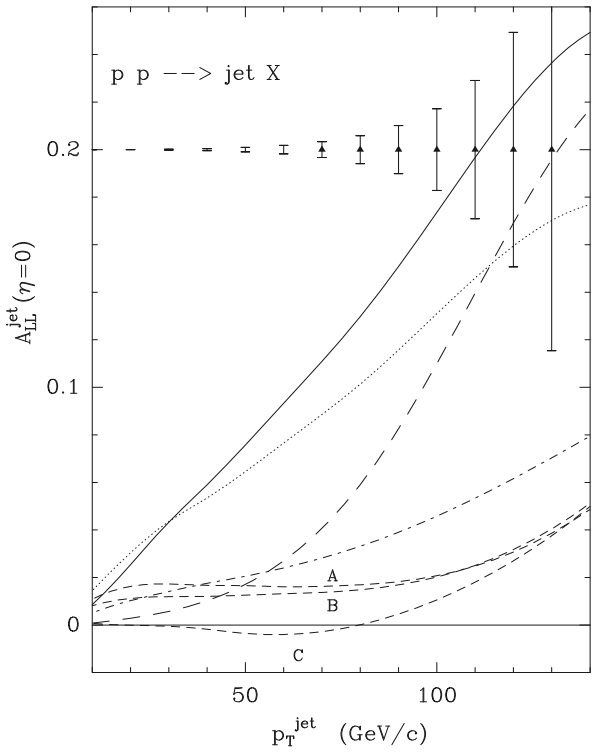

Fig. 2. The double helicity asymmetry $A_{\mathrm{LL}}^{\mathrm{jet}}(\eta = 0)$ at $\eta = 0$ versus $p_{\mathrm{T}}^{\mathrm{jet}}$ for $\sqrt{s} = 500\,\mathrm{GeV}$ calculated with different parton densities. (Curve labels as in Fig. 1.) (Taken from Ref. [10].)

case. In principle one should take into account gluon-gluon (GG), gluon-quark (Gq) and quark-quark (qq) scatterings. Although these subprocesses cross sections are not so much different, after convolution with the appropriate parton densities (see Eq. (2)), they lead to very distinct contributions to the hadronic spin-average cross section. Here we will restrict ourselves to the double helicity asymmetry $A_{\mathrm{LL}}^{\mathrm{jet}}$ for single jet production and in order to clarify the interpretation of our results below, let us recall some simple dynamical features. In the very low $p_{\mathrm{T}}^{\mathrm{jet}}$ region, say $p_{\mathrm{T}}^{\mathrm{jet}} \sim 10\,\mathrm{GeV}/c$ or so, GG scattering dominates by far, but its contribution drops down very rapidly with increasing $p_{\mathrm{T}}^{\mathrm{jet}}$. In the medium $p_{\mathrm{T}}^{\mathrm{jet}}$ range, say $20\ \mathrm{GeV}/c < p_{\mathrm{T}}^{\mathrm{jet}} < 80\,\mathrm{GeV}/c$ or so, Gq scattering dominates and then decreases for large $p_{\mathrm{T}}^{\mathrm{jet}}$, to be overcome by qq scattering. Of course these are rough qualitative considerations and accurate numerical estimates for the relative fractions of these different contributions depend strongly on the parton densities one uses. Let us look

at $A_{\rm LL}^{\rm jet}(\eta = 0)$ and, from the above discussion, we see that in the medium $p_{\rm T}^{\rm jet}$ range where Gq scattering dominates, $A_{\rm LL}^{\rm jet}(\eta = 0)$ should have a trend similar to $A_{\rm LL}^{\gamma}(\eta = 0)$, with perhaps a magnitude reduced by a factor two, since about half of the jet cross section is due to GG and qq scatterings. This is what we see approximately in Fig. 2, where we present the numerical results for $A_{\rm LL}^{\rm jet}(\eta = 0)$ at $\sqrt{s} = 500$ GeV, which should be compared to Fig. 1. We have also indicated the statistical errors which are extremely small in this case, because of the huge event rates.

4. How to pin down $\Delta q(x, Q^2)$ and $\Delta\bar{q}(x, Q^2)$?

Let us now consider, for the reaction $pp \to W^{\pm}X$, the parity violating single helicity asymmetry $A_{\rm L}$ defined in Eq. (6). In the Standard Model, the W gauge boson is a purely left-handed object and this asymmetry reads simply for $W^{\pm}$ production

$$A_{\rm L}^{W^+}(y) \,=\, \frac{\Delta u(x_a, M_W^2)\, \bar{d}(x_b, M_W^2) \,-\, (u \leftrightarrow \bar{d})}{u(x_a, M_W^2)\, \bar{d}(x_b, M_W^2) \,+\, (u \leftrightarrow \bar{d})}\,, \tag{8}$$

assuming the proton a is polarized. Here we have $x_a = \sqrt{\tau}e^{y}$, $x_b = \sqrt{\tau}e^{-y}$ and $\tau = M_W^2/s$. For W^- production the quark flavors are interchanged $(u \leftrightarrow d)$. The calculation of these asymmetries is therefore very simple and the results are presented in Figs. 3, 4 at $\sqrt{s} = 500$ GeV, for different sets of distributions. As first noticed in Ref. [4], the general trend of $A_{\rm L}$ can be easily understood as follows : at $y = 0$ one has

$$A_{\rm L}^{W^+} \,=\, \frac{1}{2}\left(\frac{\Delta u}{u} \,-\, \frac{\Delta\bar{d}}{\bar{d}}\right) \qquad \text{and} \qquad A_{\rm L}^{W^-} \,=\, \frac{1}{2}\left(\frac{\Delta d}{d} \,-\, \frac{\Delta\bar{u}}{\bar{u}}\right)\,, \tag{9}$$

evaluated at $x = M_W/\sqrt{s} = 0.164$, for $y = -1$ one has

$$A_{\rm L}^{W^+} \,\sim\, -\,\frac{\Delta\bar{d}}{\bar{d}} \qquad \text{and} \qquad A_{\rm L}^{W^-} \,\sim\, -\,\frac{\Delta\bar{u}}{\bar{u}}\,, \tag{10}$$

evaluated at $x = 0.059$ and for $y = +1$ one has

$$A_{\rm L}^{W^+} \,\sim\, \frac{\Delta u}{u} \qquad \text{and} \qquad A_{\rm L}^{W^-} \,\sim\, \frac{\Delta d}{d}\,, \tag{11}$$

evaluated at $x = 0.435$.

Therefore these measurements will allow a fairly clean flavor separation, both for quarks and antiquarks, for some interesting ranges of x values. We see in Fig. 3 that $A_{\rm L}^{W^+}$, which is driven by the u and $\bar{d}$ polarizations, leads

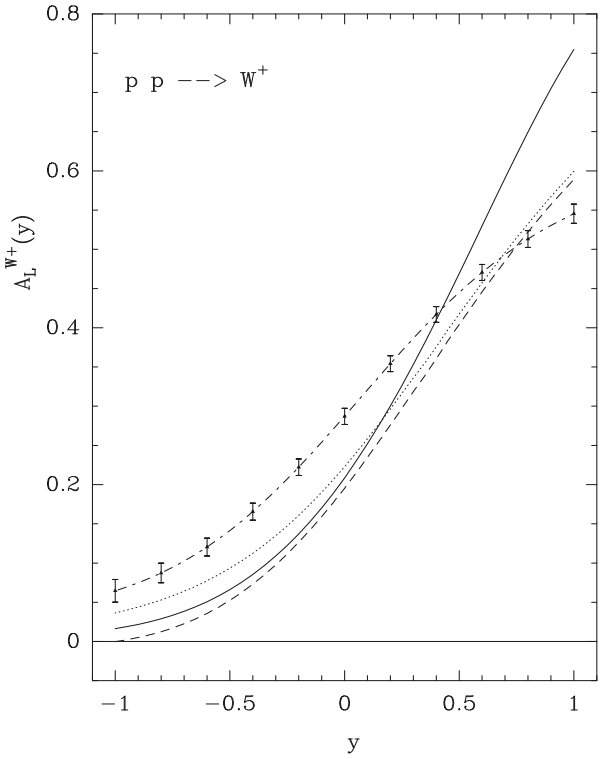

Fig. 3. The parity violating asymmetry $A_{\rm L}^{W^+}(y)$ versus y for $\sqrt{s} = 500\,\text{GeV}$ (taken from Ref. [10]) calculated with different parton densities (curve labels as in Fig. 1).

to similar predictions for all cases. This is mainly due to our knowledge of $\Delta u/u$, except for $x \geq 0.3$ where it comes out to be larger for the set proposed in Ref. [5]. In Fig. 4, for $A_{\rm L}^{W^-}$ which is sensitive to the d and $\bar{u}$ polarizations, we see that the various predictions lead to the same general trend, with some differences in magnitude due to a large uncertainty in the determination of $\Delta d/d$. Also in Ref. [5], one has assumed a larger negative $\Delta\bar{u}/\bar{u}$, which is reflected in the behaviour near $y = -1$. The statistical errors have been calculated with a rapidity resolution $\Delta y = 0.2$ and taking into account only the events from the leptonic decay modes. They are smaller for W^+ production which has larger event rates.

5. How to measure $h_1^{q,\bar{q}}(x, Q^2)$?

The existence of $h_1^q(x)$ for quarks ($h_1^{\bar{q}}$ for antiquarks) was first detected in a systematic study of the Drell–Yan process with polarized beams [11] and some of its relevant properties were discussed later in various papers [12–14].

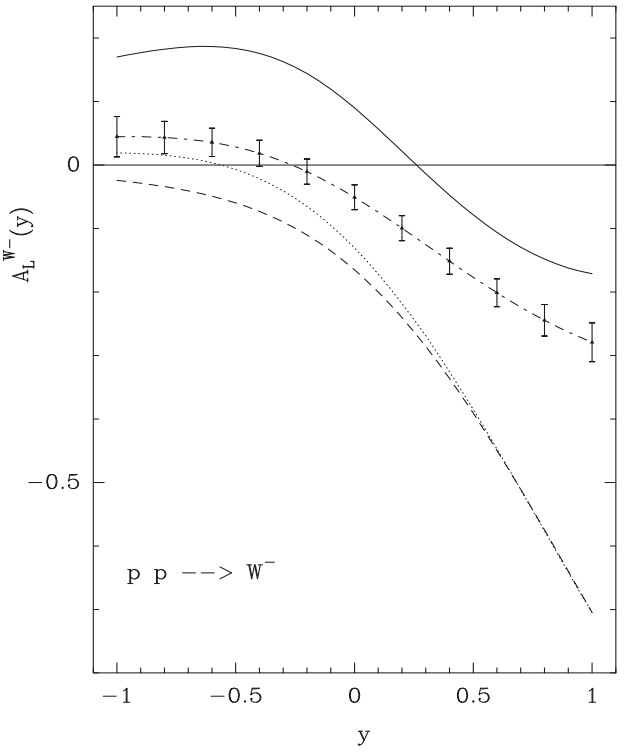

Fig. 4. Same as Fig. 3 for W^- production.

Pretty much like $q(x)$ and $\Delta q(x)$, the transversity distributions $h_1^{q,\bar{q}}(x)$ are of fundamental importance for our understanding of the nucleon structure and they are all leading-twist distributions. Due to scaling violations, these quark distributions depend also on the scale Q and their Q^2-behavior is predicted by the QCD evolution equations. They are different in the three cases but, due to lake of time, we will not discuss here this important question [15,16]. We recall that $h_1^q(x,Q^2)$ (or $h_1^{\bar{q}}(x,Q^2)$) are not simply accessible in DIS because they are in fact chiral-odd distributions, contrarily to $q(x,Q^2)$ and $\Delta q(x,Q^2)$ which are chiral-even [14]. However they can be extracted from polarized Drell–Yan processes with two transversely polarized proton beams. For lepton pair production $pp \to \ell^+\ell^- X$ ($\ell = e,\mu$) mediated by a virtual photon $\gamma^\star$, the double transverse-spin asymmetry $A_{\rm TT}^{\gamma^\star}$ defined, similarly to Eq. (3), as $A_{\rm TT} = d\delta\sigma/d\sigma$, reads

$$A_{\rm TT}^{\gamma^\star} = \widehat{a}_{\rm TT} \frac{\sum_q e_q^2 h_1^q(x_a,M^2) h_1^{\bar{q}}(x_b,M^2) + (a \leftrightarrow b)}{\sum_q e_q^2 q(x_a,M^2)\bar{q}(x_b,M^2) + (a \leftrightarrow b)}, \tag{12}$$

where $\widehat{a}_{\rm TT}$ is the partonic asymmetry calculable in perturbative QCD and M is the dilepton mass. The rapidity y of the dilepton is $y = x_a - x_b$, and for $y = 0$ one has $x_a = x_b = M/\sqrt{s}$. Note that this is a leading-order expression, which can be used to get a first estimate of $A_{\rm TT}^{\gamma\star}$ from different theoretical results for h_1^q and $h_1^{\bar{q}}$. If the lepton pair is mediated by a Z gauge boson, one has a similar expression for $A_{\rm TT}^Z$ [17], namely

$$A_{\rm TT}^Z = \frac{\sum_q (b_q^2 - a_q^2) h_1^q(x_a, M_Z^2) h_1^{\bar{q}}(x_b, M_Z^2) + (a \leftrightarrow b)}{\sum_q (b_q^2 + a_q^2) q(x_a, M_Z^2) \bar{q}(x_b, M_Z^2) + (a \leftrightarrow b)}, \tag{13}$$

where a_q and b_q are the vector and axial couplings of the flavor q to the Z. However in the case of $W^\pm$ production one expects $A_{\rm TT}^W = 0$, because the W gauge boson is a pure left-handed object (*i.e.*, $a_q = b_q$), which does not allow a left-right interference effect associated to the existence of $h_1^{q,\bar{q}}$ [17]. We show in Fig. 5 some predictions, at leading and next to leading orders, for $A_{\rm TT}$, together with some expected statistical errors, where one sees a characteristic effect in the Z mass region. The asymmetry is only a few percents, due to the smallness of $h_1^{\bar{q}}$, but this is a real challenge for the experiment.

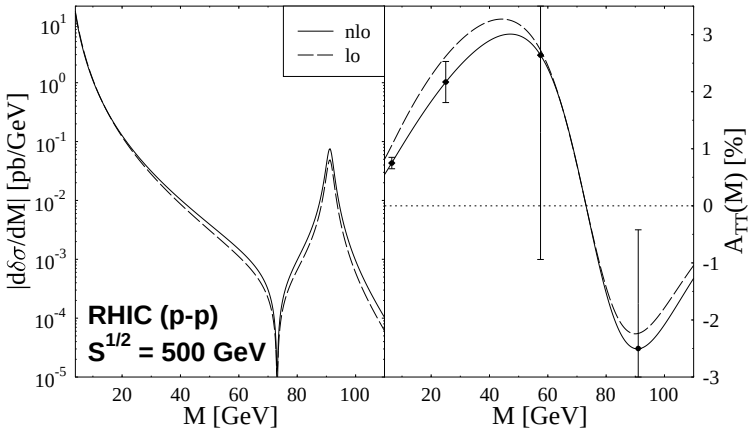

Fig. 5. NLO and LO maximal polarized Drell–Yan cross section ($|d\delta\sigma|$) and asymmetry($A_{\rm TT}$) for RHIC at $\sqrt{s} = 500\,\text{GeV}$ assuming the maximum luminosity. (Taken from Ref. [16].)

6. How to uncover new parity violation effects?

Let us consider again one-jet inclusive production. As discussed in Section 3, the cross section is dominated by the pure QCD subprocesses GG, Gq

and qq scatterings, but the existence of the electroweak (EW) interaction, via the effects of the $W^{\pm}, Z$ gauge bosons, adds to it, a small contribution. Consequently, the parity violating asymmetry $A_{\rm LL}^{\rm PV}$ defined in Eq. (7) and resulting from the QCD-EW interference is non-zero, as shown in Fig. 6 (see curve SM) and has a small structure near $E_{\rm T} = M_{W,Z}/2$. Now if we introduce a new contact interaction, belonging purely to the quark sector and normalized to a certain compositeness scale Λ, under the form

$$\mathcal{L}_{qqqq} = \varepsilon \frac{g^2}{8\Lambda^2} \bar{\Psi}\gamma_\mu(1-\eta\gamma_5)\Psi.\bar{\Psi}\gamma^\mu(1-\eta\gamma_5)\Psi \ , \tag{14}$$

where Ψ is a quark doublet and $\varepsilon = \pm 1$. If parity is not conserved $\eta = \pm 1$ and we show in Fig. 6, how the SM prediction will be affected by such a new interaction assuming $\Lambda = 1.6\,\text{GeV}$. As expected, the errors are large in the high $E_{\rm T}$ region, but if the observation of such a signal is confirmed, it will be extremely important.

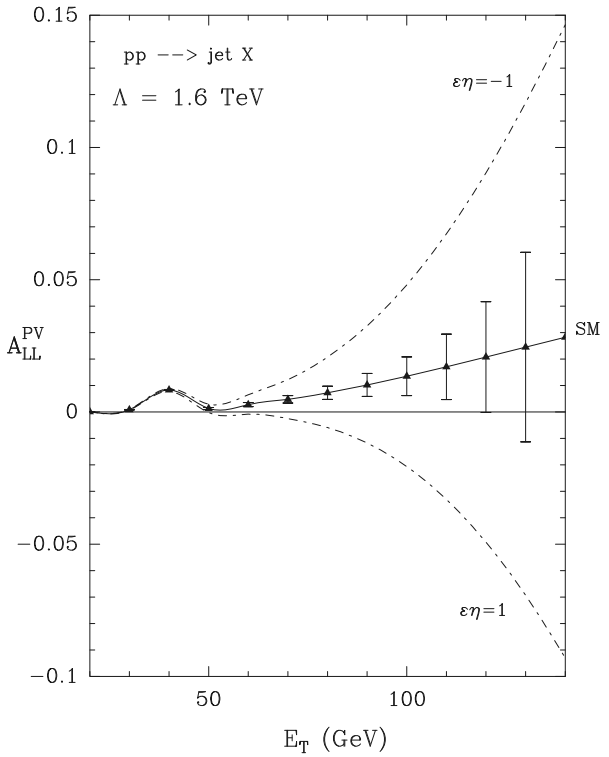

Fig. 6. $A_{\rm LL}^{\rm PV}$ versus $E_{\rm T}$ at RHIC for $\sqrt{s} = 500\,\text{GeV}$, for $\Lambda = 1.6\text{TeV}$. (Dashed curve corresponds to $\varepsilon\eta = -1$, dot-dashed curve to $\varepsilon\eta = +1$ and solid curve, SM, is the pure QCD-EW interference.) (Taken from Ref. [18]).

It is my pleasure to thank Marek Jeżabek for the invitation and all the other organizers for setting up this excellent conference in such a pleasant and stimulating atmosphere.

REFERENCES

[1] G. Altarelli, *Acta Phys. Pol.* **B29**, 1145 (1998), this issue.

[2] See *e.g.*, FNAL-E704 Collaboration, A. Bravar *et al.*, *Phys. Rev. Lett.* **77**, 2626 (1996) and references therein.

[3] C. Bourrely, J. Soffer, F.M. Renard, P. Taxil, *Phys. Rep.* **177**, 319 (1989), and the errata preprint CPT-87/P.2056, January 1991; see also P. Taxil, *Riv. Nuovo Cim.* **16**, No.11, 1 (1993).

[4] C. Bourrely, J. Soffer, *Phys. Lett.* **B314**, 132 (1993).

[5] C. Bourrely, J. Soffer, *Nucl. Phys.* **B445**, 341 (1995).

[6] C. Bourrely, F. Buccella, O. Pisanti, P. Santorelli, J. Soffer, preprint CPT-96/PE.3327, DSF-T96/17, to appear in the proceedings of the Fundamental Structure of Matter, Ouranoupoulis, Greece, May 28–31, 1997, Ed. A. Nicolaidis.

[7] T. Gehrmann, W.J. Stirling, *Phys. Rev.* **D53**, 6100 (1996).

[8] M. Glück, E. Reya, M. Stratmann, W. Vogelsang, *Phys. Rev.* **D53**, 4775 (1996).

[9] H.Y. Cheng, H.H. Liu, *Phys. Rev.* **D53**, 2380 (1996).

[10] J. Soffer, J.M. Virey, *Nucl. Phys.* **B509**, 297 (1998).

[11] J.P. Ralston, D.E. Soper, *Nucl. Phys.* **B152**, 109 (1979).

[12] X. Artru, M. Mekhfi, *Z. Phys.* **C45**, 669 (1990).

[13] J.L. Cortes, B. Pire, J.P. Ralston, *Z. Phys.* **C55**, 409 (1992).

[14] R.L. Jaffe, X. Ji, *Phys. Rev. Lett.* **67**, 552, (1991); *Nucl. Phys.* **B375**, 527 (1992).

[15] C. Bourrely, J. Soffer, O.V. Teryaev, preprint CPT-97/P.3538 (*Phys. Lett.* **B**, to appear).

[16] O. Martin, A. Schäfer, M. Stratmann, W. Volgelsang, preprint CERN-TH/97-270, October 1997.

[17] C. Bourrely, J. Soffer, *Nucl. Phys.* **B423**, 329 (1994).

[18] P. Taxil and J.M. Virey, *Phys. Lett.* **B364**, 181 (1995).